EPJ manuscript No.
(will be inserted by the editor)

Magnetic anisotropy and low-frequency dielectric response of weak ferromagnetic phase in κ-(BEDT-TTF)$_2$Cu[N(CN)$_2$]Cl, where BEDT-TTF is Bis(ethylenedithio)tetrathiafulvalene

M. Pinterić[1,2], M. Miljak[1], N. Biškup[1], O. Milat[1], I. Aviani[1], S. Tomić[1] , D. Schweitzer[3], W. Strunz[4], and I. Heinen[4]

[1] Institute of Physics, P. O. Box 304, HR-10000 Zagreb (Croatia)
[2] Faculty of Civil Engineering, University of Maribor, SLO-2000 Maribor (Slovenia)
[3] 3. Physikalisches Institut, Universität Stuttgart, D-70550 Stuttgart (Germany)
[4] Anorganisch-chemiches Institut, Universität Heidelberg, D-69120 Heidelberg (Germany)

Received: date / Revised version: date

Abstract. We report a detailed characterization of the magnetism and AC transport in single crystals of the organic conductor κ-(BEDT-TTF)$_2$Cu[N(CN)$_2$]Cl by means of magnetic anisotropy measurements and low-frequency dielectric spectroscopy. Magnetic anisotropy obeys Curie-Weiss law with negative Curie-Weiss temperature in the temperature range 300 K - 70 K. An antiferromagnetic transition with concomitant canted antiferromagnetic state is established at 22 K. A large hysteresis in the spin-flop transition and magnetic field reversal of the weak ferromagnetic magnetization are documented for the first time. A broad dielectric relaxation mode of moderate strength ($\Delta\varepsilon \approx 3 \cdot 10^3$) emerges at 32 K, and weakens with temperature. The mean relaxation time, much larger than that expected for single-particle excitations, is thermally activated in a manner similar to the DC conductivity and saturates below 22 K. These features suggest the origin of the broad relaxation as an intrinsic property of the weak ferromagnetic ground state. We propose a charged domain wall in a random ferromagnetic domain structure as the relaxation entity. We argue that the observed features might be well described if Dzyaloshinsky-Moriya interaction is taken into account. A Debye relaxation with similar temperature dependence was also observed and seems to be related to an additional ferromagnetic-like, most probably, field-induced phase. We tentatively associate this phase, whose tiny contribution was sample dependent, with a Cu^{2+} magnetic subsystem.

PACS. 74.70.Kn Organic superconductors – 72.15.Nj Collective modes – 75.30.Gw Magnetic anisotropy

1 Introduction

The magnetic properties of organic conductors and superconductors have been extensively studied both experimentally and theoretically in the last twenty years [1,2]. It is intriguing that magnetic insulators are found in the vicinity of superconductors not only for the Bechgaard salts but also for the κ phase BEDT-TTF (abbreviated ET) compounds. The competition between these two ground states is governed by pressure and/or the choice of the anion. In the former, the electronic system is quasi-one-dimensional and the nesting of an open Fermi surface leads to a metal-insulator phase transition and spin-density wave (SDW) ground state. In the latter, the quasi-two-dimensional nature of the electronic system is expected to prevent nesting and keep the metallic state down to low temperatures and the superconducting ground state. It is therefore remarkable that a magnetic insulating state in the proximity of superconductivity, is found recently in the κ-(BEDT-TTF)$_2$Cu[N(CN)$_2$]Cl material which possesses the highest superconducting critical temperature under slight pressure among these anisotropic systems [3,4]. The pressure which suppresses the magnetic state and stabilizes superconductivity is only 300 bars, the smallest ever encountered in the organic salts. While the nature and properties of spin density waves are well understood, not much is known about the origin and features of the magnetic state in κ phase BEDT-TTF compounds. A full characterization of the magnetic state is also important for the understanding of superconductivity in this class of materials.

κ-(BEDT-TTF)$_2$Cu[N(CN)$_2$]Cl material belongs to the κ-(ET)$_2$X (X = polymerized anion) class of ET systems in which orthogonally aligned ET dimers form 2D conducting layers sandwiched between the polymerized anion layers. Its unit cell contains two ET layers (i.e. 4 dimers) and 4 anions. The donor molecules form face-to-face orthogonal dimers which are rotated by ca. 45 degrees with respect to the unit cell axes (a and c). The copper atoms complete their trigonal coordination environment with a bond to a terminal chlorine atom. The 2D layers

Correspondence to: stomic@ifs.hr

of the organic donor molecules lie in the crystallographic ac-plane, which coincides with the large face of the crystal, and these layers are alternatively separated by anion layers along the b axis.

The first magnetization measurements performed by Welp et al. [5] claimed an antiferromagnetic (AF) transition at 45 K and a weak ferromagnetic state below 22 K. Later, the results of NMR measurements of Miyagawa et al. [6] showed a large enhancement of the spin-lattice relaxation rate below 50 K and a sharp peak at 27 K. The former was interpreted to be due to the antiferromagnetic spin fluctuations, and the latter as a sign of an antiferromagnetic phase transition. The established order is commensurate with the underlying lattice and possesses a rather large moment of (0.4-1.0) μ_B/dimer. In addition, magnetization measurements by the same authors showed that weak ferromagnetism appears below 23 K due to the canting of spins. As in this temperature range, a finite energy gap is already opened in the charge degrees of freedom, Miyagawa et al. suggested that the magnetic ordering of localized spins driven by electron-electron correlations was in origin of the observed phase transition. Kino et al. [7] proposed a theoretical model in which the AF ordering with the large magnetic moment and a simultaneous metal-to-insulator phase transition is predicted as the effect of a strong enough on-site Coulomb interaction within the Hartree-Fock approximation. However, the origin of spin canting remained unclear.

In order to get more information about the low-temperature state in κ-(BEDT-TTF)$_2$Cu[N(CN)$_2$]Cl material, we have performed measurements of the magnetic anisotropy and the low-frequency dielectric response. We show that the phenomena of magnetism and the associated low-frequency dielectric relaxation are more complex than what had been considered. Our data give clear evidence of a canted antiferromagnetic state established below 22 K. A large hysteresis of the spin-flop transition and magnetic field reversal of the ferromagnetic moment are observed for the first time. The observed dielectric response data give evidence of a collective mode contribution to the dielectric properties which might be attributed to domain walls in a ferromagnetic domain structure. We suggest that the features observed could be accounted for taking into consideration the Dzyaloshinsky-Moriya interaction. Our arguments are based on symmetry considerations. The Currie-Weiss high temperature behaviour of the anisotropy, an additional non-linear magnetization and Debye relaxation mode are tentatively associated with a Cu^{2+} ion subsystem.

2 Experimental and results

The rhombic plate-like single crystals used in this study were about 0.2 mm^3 in size. Crystallographic orientation of one of two crystals used in the magnetic anisotropy measurements was determined by taking two oscillation XRD patterns (Ni-filtred Cu$_{K\alpha}$; Weissenberg camera) with (a) oscillation axis parallel to the longer edge - assigned as the [102] lattice direction, and (b) oscillation axis perpendicular to the shorter edge - assigned as the [101] direction. The b = [010] axis being perpendicular to the plane of the sample, while the in-plane principal axes were unambiguously identified as a = [100] - parallel to the line bisecting the obtuse angle (110°) and c = [001] - parallel to the line bisecting the sharp angle (70°). Single crystal magnetic anisotropy was measured by the torque method from 300 K to 4.2 K in fields up to 8 kOe. The torque ($\mathbf{\Gamma}$) is defined as $\mathbf{\Gamma} = \mathbf{M} \times \mathbf{H}$, where $\mathbf{M}$ and $\mathbf{H}$ are the magnetization and magnetic field vector, respectively. The equations (1) and (2) give the torque in the paramagnetic and ferromagnetic state, respectively.

$$\Gamma_{para} = \frac{m}{2M_{mol}} \cdot \Delta\chi \cdot H^2 \cdot \sin(2\varphi) \tag{1}$$

$$\Gamma_{ferro} = \frac{m}{M_{mol}} \cdot M_f \cdot H \cdot \sin(\varphi) \tag{2}$$

m is the sample mass, M_{mol} is molecular weight and M_f is the permanent magnetization. $\Delta\chi$ and φ are the anisotropy of the susceptibility and the angle between the magnetic field orientation and the chosen crystallographic directions of the sample, respectively. In our measurements the angle φ was the angle in the crystallographic bc-plane and/or ab-plane defined by sample and field orientation. The anisotropy and the ferromagnetic magnetization were determined as a function of temperature, and the strength and/or orientation of the magnetic field. The complex conductance $(G(\omega), B(\omega))$ was measured by a Hewlett Packard HP4284A impedance analyzer (ν = 20Hz$-$1MHz) in the two-probe configuration in the temperature range between 10 K and 40 K. In order to determine the quality of the contacts, we have performed two independent checks. First, only two contacts were attached to two opposite faces of the crystal, in order to minimize stray capacitances for the complex conductance measurements. The DC resistance measurements were performed using a standard DC technique or Keithley 617 electrometer in V-I mode. In addition, the DC conductance G_0 obtained from $G(\omega)$ at low frequencies using HP impedance analyzer was close to the $1/R$ obtained using DC technique. Later, two additional contacts were mounted, and the DC resistance measurements were performed in the four probe configuration. The observed $\log R$ vs. T curves were essentially the same. At temperatures lower than 40 K, the higher limit of the contact resistance was estimated to be smaller than 20 % of the sample resistance. Second, Cole-Cole plots are also considered as helpful in determining the quality of contacts, since additional deformed arcs appear for each additional process such as capacitive coupling between the sample and the contacts. The Cole-Cole plots for studied samples were free from such spurious influences. Further, we have verified, by performing "open-circuit measurements", that the stray capacitances do not influence the real part of the conductivity in the frequency window 20 Hz - 600 kHz and in the temperature range of our study. Finally, for the AC signal levels employed in the range between 5 mV and 100 mV we have always essentially obtained the same result.

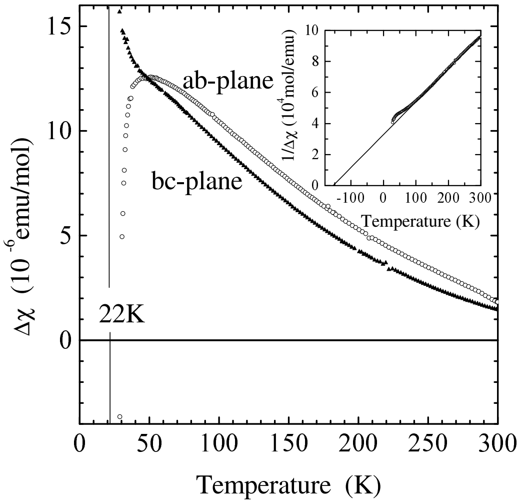

Fig. 1. Temperature dependence of the susceptibility anisotropy in the ab and in the bc-plane. Solid line (Inset) indicates a Curie-Weiss fit.

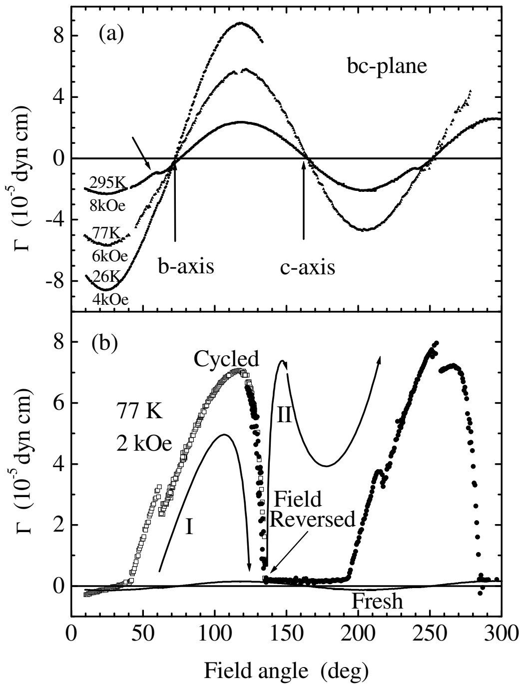

Fig. 2. (a) Torque vs. angle in the bc-plane at three temperatures. (b) Torque anomaly associated with an additional non-linear contribution indicated by an arrow in (a) is shown for one single crystal at 77 K (fresh) and after temperature cycling: run I and II with **H** and −**H** (reversed field), respectively.

Fig. 1 shows the anisotropy of the susceptibility as a function of temperature. Note the difference in the behaviour of $\Delta\chi$ in the ab and bc-plane below 50 K. The former continues to increase but with a larger rate, while the latter displays a maximum and falls down rapidly. We fitted the data of $\Delta\chi$ between 300 K and 70 K with $\Delta\chi(T) = \Delta\chi_0 + \Delta\chi_{cw}$, where $\Delta\chi_0$ is the temperature independent term and $\Delta\chi_{cw} \propto C/(T - \theta_{cw})$ is the temperature-dependent Curie-Weiss term (see Inset of Fig. 1). Here C is the Curie constant and θ_{cw} is the Curie-Weiss temperature. The $\Delta\chi_0$ is estimated at about $9 \cdot 10^{-6}$ emu/mole and it can come either from molecular diamagnetism or Van Vleck (orbital) contribution. The Curie-Weiss temperature $\theta_{cw} = -160$ K has a negative sign, which is usually interpreted as an indication of an antiferromagnetic interaction. However, we point out that the Curie-Weiss behaviour of the anisotropy is not in accordance with the susceptibility behaviour. That is, the static susceptibility [8,9], as well as the spin susceptibility measured by ESR [10], remains almost constant down to 100 K, and decreases gradually at lower temperatures. In Fig. 2(a) we show the angular dependence of the torque in the bc-plane measured at 295 K, 77 K and 26 K. The torque dependencies observed are typical of a paramagnetic state (see Eq.(1)). In addition to the linear magnetization contribution of the $\sin(2\varphi)$ form, there is clearly, even at RT, a small but non-linear contribution of unusual angular and field dependence which persists in the entire temperature range which was measured. This non-linear term is manifested mostly as a small angular shift of the torque curve, but it also causes the deviation of the otherwise regular $sin(2\varphi)$ function. This effect is visible in Fig. 2(a) in the vicinity of the principal susceptibility axis ($\Gamma = 0$) which corresponds to the crystallographic b-axis, and is present for both mutually perpendicular sample orientations. The b-axis was always in the magnetic field rotation plane. One should note the 180 degrees symmetry of the anomaly. For the sake of curiosity we show how this torque component became anomalously enhanced for one sample after repeated temperature cycling between RT and 77 K (see Fig. 2(b)). While the amplitude of this non-linear magnetization is sample (batch) dependent, we have not observed any change in the functional form of the field dependence. Furthermore, the existence of this component does not affect the low-temperature canted antiferromagnetic state.

An AF transition is established at 22 K as revealed in the plot of $\Delta\chi$ versus temperature in the bc-plane shown in Fig. 3. Fig. 4 shows the torque versus the squared field at 21.5 K for the field orientation close to the b axis. The data obtained confirm that the easy axis is parallel to the b axis, and reveal the existence of a large hysteresis in the spin-flop transition. We get $H_{sf1} = 2$ kOe and $H_{sf2} = 1$ kOe for the spin-flop fields when the field is swept up and down, respectively. We also note that $T = 21.5$ K was the highest temperature at which we observed the spin-flop transition. In Fig. 5 we show the angular dependence of the torque in the bc-plane measured at 4.2 K. While torque angular dependencies measured above 26 K are typical of the paramagnetic state, a sinusoidal dependence with doubled periodicity observed at 4.2 K provides direct evidence of the existence of ferromagnetic magnetization (see Eq.(2)). It should be stressed that we do not find the ferromagnetic magnetization when the torque is measured in the ab-plane, where only the contribution of the paramagnetic component is visible. The magnitude of the torque observed in the field of 100 Oe

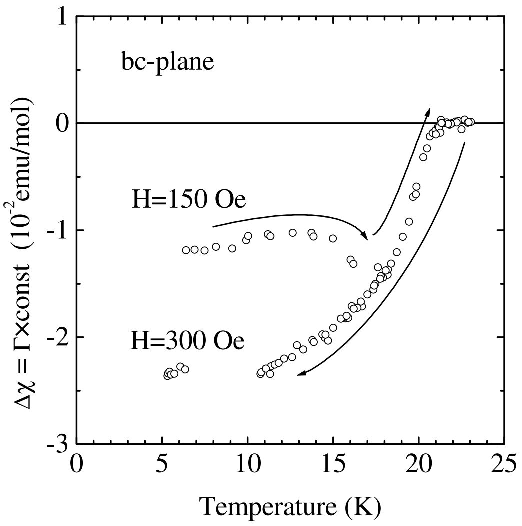

Fig. 3. Temperature dependence of the susceptibility anisotropy in the bc-plane through the antiferromagnetic phase transition. Arrows indicate cooling down at $H = 300$ Oe and subsequent warming up at $H = 150$ Oe.

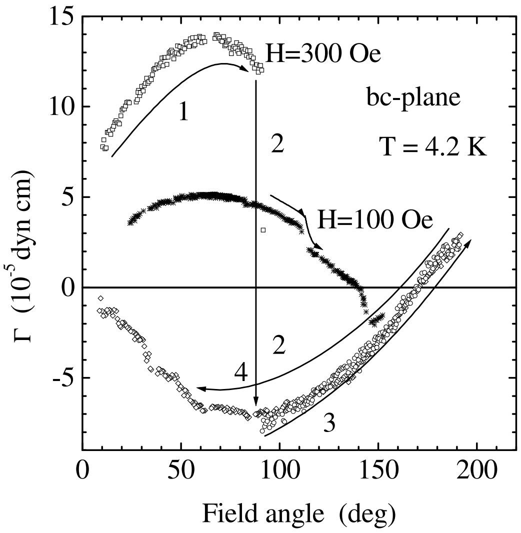

Fig. 5. Torque vs. angle in the bc-plane at 4.2 K for two field values. Arrows (1,2,3) and (4) indicate the increasing and decreasing fields ($H = 300$ Oe), respectively.

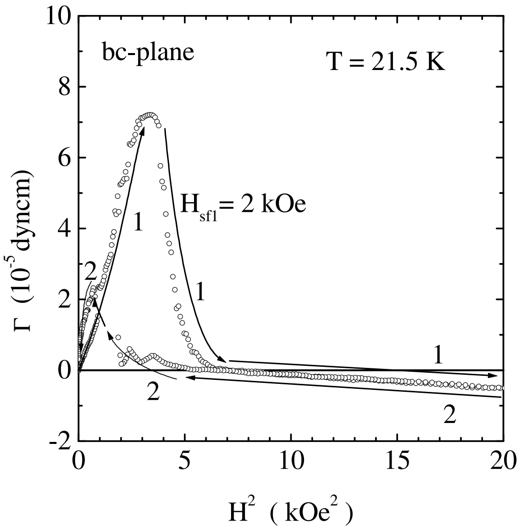

Fig. 4. Torque vs. field squared at $T = 21.5$ K for **H** close to the b axis in the bc- plane. Arrows (1) and (2) indicate the increasing and decreasing fields, respectively.

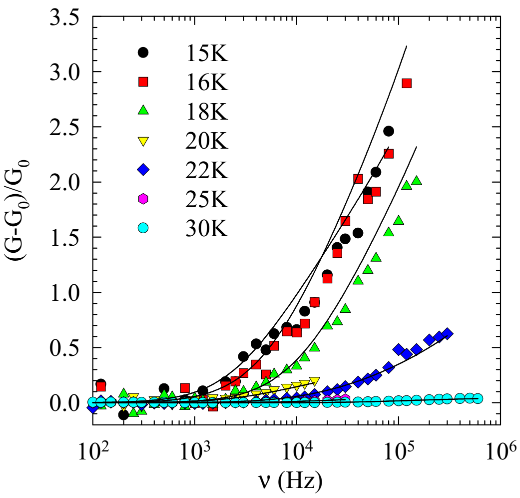

Fig. 6. The real part of the conductivity normalized to the DC value ($(G - G_0)/G_0$) versus frequency for a temperature range between 30 K and 15 K. Full lines are fits to the HN form.

is $\Gamma \approx 5 \cdot 10^{-5}$ dyncm. This value corresponds to the magnetization of $M = \Gamma/H \approx 5 \cdot 10^{-7}$ emu/mole. Taking $M_{mol} \approx 1000$ g/mole for the molecular mass and $\rho \approx 2.2\,\mathrm{g/cm^3}$ as the specific density we get the ferro magnetization $M_f \approx 2 \cdot 10^{-9}\,\mathrm{emu/cm^3}$. The estimated number of spins giving this magnetization is then $N_f \approx 5 \cdot 10^{13}$. As the total number of spins (s=1/2) in the sample is about $N_{tot} \approx 6 \cdot 10^{16}$, we get the canting angle of the order of 1/1000 rad i.e. $6 \cdot 10^{-2}$ degrees. Finally, there is a drop in the torque of the order of $\Delta\Gamma/\Gamma \approx 33\%$ which occurs for the field $H = 100$ Oe at 4.2 K. At the same temperature, a three times larger field $H = 300$ Oe was sufficiently high in order to switch the magnetization from $M \approx 4 \cdot 10^{-7}$ emu/mole to $M \approx -2.3 \cdot 10^{-7}$ emu/mole. The magnetization keeps the reversed sign until the magnetic field is turned off.

The real part of the conductivity normalized to the DC value $(G(\nu) - G_0)/G_0$ as a function of frequency at a few selected temperatures is shown in Fig. 6. At $T > 32$ K a frequency independent conductivity is found. Below 32 K we observe a clear crossover from frequency-independent conductivity at low frequencies to a frequency dependent component at higher frequencies. It should be noted that an enhanced AC conductivity increases in significance and starts at lower frequencies as the temperature lowers. Dielectric functions were extracted from the conductivity using the relations $\varepsilon'(\omega) = B(\omega)/\omega$, and $\varepsilon''(\omega) = (G(\omega) - G_0)/\omega$, where G_0 is the DC conductivity obtained from the $G(\omega)$ measured at low frequencies

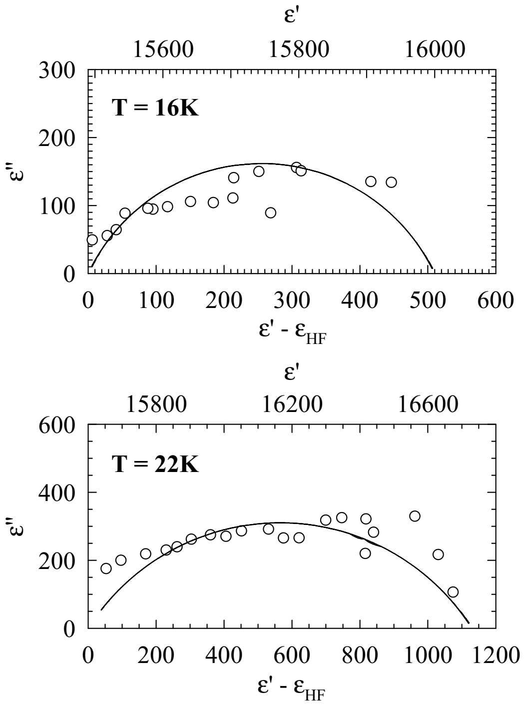

Fig. 7. Cole-Cole plots of the dielectric response at two selected temperatures. Full lines are from fits to the HN form.

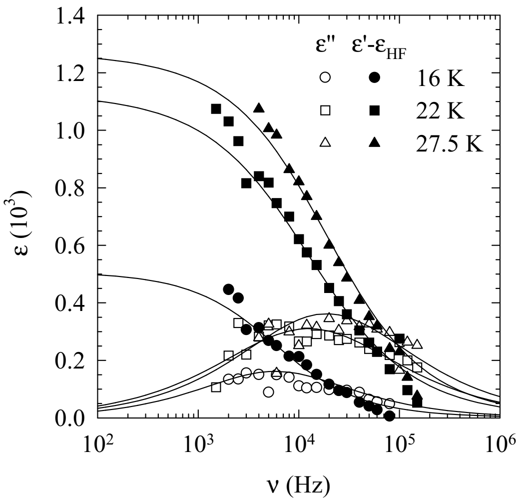

Fig. 8. Frequency dependence (log scale) of the real and imaginary parts of the dielectric function for three representative temperatures. Full lines are from fits to the HN form.

where $G(\omega)$ was independent of ω ($\omega = 2\pi\nu$). The initial analysis of the dielectric function was performed by the inspection of Cole-Cole plots which are presented in Fig. 7. The intersection of the arcs with ε' axis at high and low ε' values, corresponding to low and high frequencies, indicates the values of the static dielectric constant ε_0 and the high frequency dielectric constant ε_{HF}, respectively. As indicated in Fig. 7, ε_{HF} is substantial compared to the strength of the relaxation process $\Delta\varepsilon = \varepsilon_0 - \varepsilon_{HF}$, and was found to correspond to the value of stray capacitance obtained in the "open-circuit" measurements. The value of the relaxation strength is moderate, of the order of 1000. Fig. 8 shows frequency domain plots of the real and imaginary part of the dielectric function at three selected temperatures. It should be noted that $\varepsilon''(\nu)$ curves move toward lower peak frequencies ($\nu_0 = \omega_0/2\pi = 1/2\pi\tau_0$) and smaller peak amplitudes with decreasing temperature without significant change in the shape. The observed dielectric response can be well fitted by the phenomenological Havriliak-Negami (HN) function

$$\varepsilon(\omega) - \varepsilon_{HF} = \frac{\Delta\varepsilon}{1 + (i\omega\tau_0)^{1-\alpha}} \tag{3}$$

This function has been widely used to describe the non-Debye character of the relaxation processes in disordered systems [11,12]. τ_0 and $1-\alpha$ are the mean relaxation time and the shape parameter which describes the symmetric broadening of the relaxation time distribution function, respectively. The dielectric data were analyzed by using two methods. In the first method we analyze the real and imaginary part of the dielectric function separately. In the second one, we analyze the dielectric function in the complex plane, so a single value for each parameter was obtained for both the real and the imaginary part of the data. The latter method is based on the same principle as the former, i.e. the least square method, the only difference being in that the experimental data and the theoretical function in the latter are treated as complex values. The full lines in Figs. 6, 7 and 8 correspond to the calculated fits. The fit parameters as a function of inverse temperature are shown in Fig. 9. The parameter $\Delta\varepsilon$ which measures the strength of the relaxation process and corresponds to the static dielectric susceptibility decreases with temperature less than one order of magnitude between 32 K and 14 K. The width of the relaxation time distribution expressed by the $(1-\alpha)$ parameter is close to 1 at 32 K. However, already below 28 K the mode broadens and the value of $(1-\alpha) \approx 0.7$ does not change significantly with temperature. The mean relaxation time τ_0 closely follows thermally activated behaviour in a manner similar to the DC conductivity in the temperature range 32 K - 25 K, and saturates below 22 K. Finally, we show representative Cole-Cole plots of the data measured on the second single crystal (Fig. 10), which reveal the existence of two relaxation modes. While the observed dielectric response of the first sample was successfully fitted to a single HN mode using the two analysis procedures described above, similar attempts to fit the data of the second sample failed. Therefore, the obvious solution was to try to fit the observed data to a formula representing a sum of two Havriliak-Negami (HN) modes. A representative frequency domain plot of the real and imaginary part of dielectric function at 25 K is shown in Fig. 11. The analysis in the complex space gave very satisfactory fits and revealed that the broader of the two existing modes is exactly the same as the one observed in the first sample. Namely, the calculated fit parameters and their temperature behaviour correspond to those found for the first crystal. In addition to this broad mode, there is a mode centred at low frequencies which is characteristic of a relaxation process with a single relax-

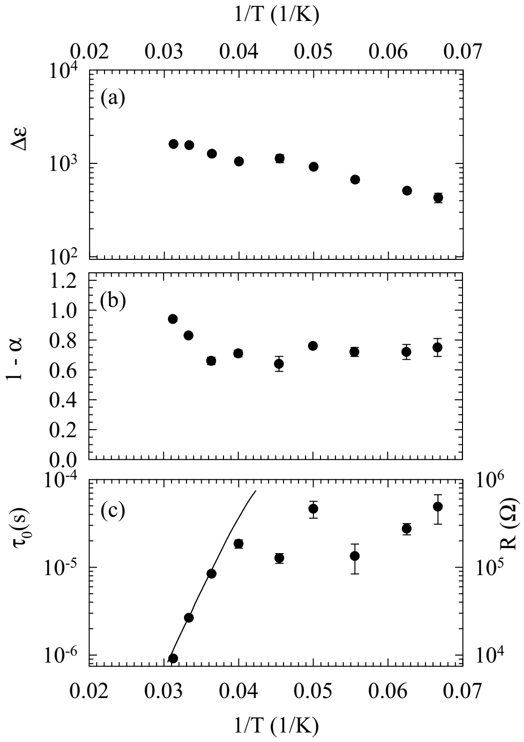

Fig. 9. (a) Relaxation strength ($\Delta\varepsilon$) vs. inverse temperature. (b) Shape parameter ($1-\alpha$) vs. inverse temperature. (c) Mean relaxation time (τ_0, full points) and DC resistance (R, full line) vs. inverse temperature.

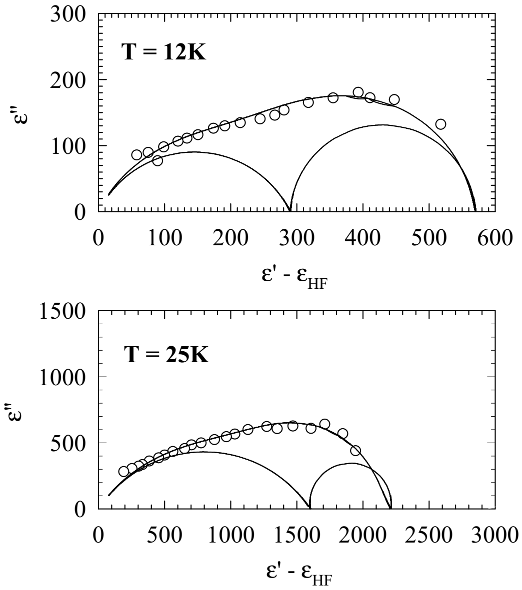

Fig. 10. Cole-Cole plots of the dielectric response at two selected temperatures for the second single crystal. Full lines are from fits to the sum of two HN forms.

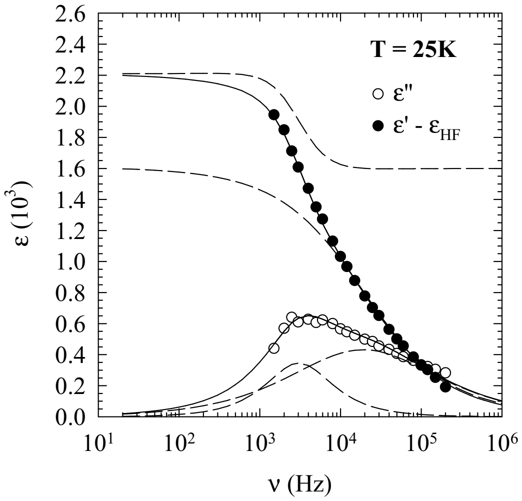

Fig. 11. Frequency dependence (log scale) of the real and imaginary parts of the dielectric function at $T = 25$ K for the second single crystal. Full lines are fits to the sum of the two HN forms. Dashed lines represent the single HN form.

ation time (Debye process). The relaxation strength and the characteristic relaxation time of the Debye mode show a qualitatively similar temperature dependence.

3 Discussion

The observed magnetic and dielectric properties of κ-(BEDT-TTF)$_2$Cu[N(CN)$_2$]Cl reveal the existence of two mutually uncorrelated magnetic subsystems which we tentatively associate with the donor (BEDT-TTF) and the acceptor chains (Cu[N(CN)$_2$]Cl), respectively. The latter might contain Cu ions in a mixed-valence state between Cu^{1+} and Cu^{2+}. We first address the properties of the former, and at the end of the paragraph we comment upon the latter.

Our anisotropy data ($\Delta\chi$) have identified the antiferromagnetic transition at $T_N = 22$ K to a canted antiferromagnetic ground state. The easy axis is confirmed to be along the crystallographic b-axis. The AF spins are canted by an angle of $6 \cdot 10^{-2}$ degrees from b-axis in such a way that the vector of ferromagnetic moment is aligned along the crystallographic c-axis. A hysteresis of the order of 1 kOe in the spin-flop transition and magnetic field reversal of the ferromagnetic magnetization are features not encountered in the standard antiferromagnets and spin density waves. The latter feature indicates the existence of a domain structure which is a well known property of magnetically ordered state. That is, when the magnetic field is absent the energy of the ferromagnetic crystal is lowered when the crystal is divided into domains with equivalent spin configurations.

The main dielectric relaxation process with the following features takes place below 32 K. The width is larger than for the Debye process and does not change with temperature below 28 K. The relaxation strength is of the order of 1000 and decreases on lowering the temperature. The characteristic relaxation time is too long to be attributed to free carriers. τ_0 is thermally activated with the activation energy close the free-carriers one in the narrow temperature range 32 K - 25 K and saturates below $T_N = 22$ K. Therefore, we are led to identify the

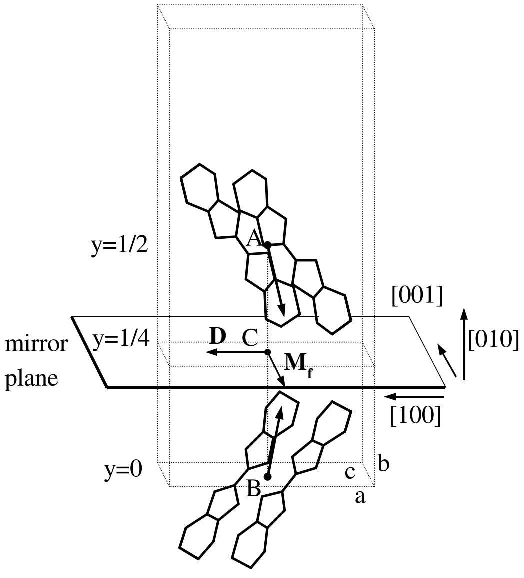

Fig. 12. Unit cell of the κ-(BEDT-TTF)$_2$Cu[N(CN)$_2$]Cl. Proposed positions of A and B sublattice magnetization are indicated. The net moment $\mathbf{M_f}$ and the vector $\mathbf{D}$ are directed along c and a axis, respectively.

origin of this relaxation as an intrinsic property of the weak ferromagnetic state established below 22 K. We propose a charged domain wall in the ferromagnetic domain structure as the relaxation entity. The broad distribution of relaxation times ($1-\alpha \approx 0.7$) might be reasonably assumed to be due to a distribution of activation energies. Then, the dielectric response is due to the activation between different metastable states over energy barriers. These metastable states correspond to local changes of the spin configuration. The length scale over which such processes occur defines the thickness of the wall and is set by the competition between relevant energies of the problem. The fact that the energy scale for the barrier heights is close to the free-carrier activation energy only above $T_N = 22$ K indicates that the free-carrier screening influences the relaxation only in the fluctuating pretransitional regime. At 22 K the relaxation time levels off. The change in the $\log \tau_0$ vs. $1/T$ plot at $T_N = 22$ K might indicate that the resistive dissipation is not the dominant dissipation mechanism in the weak ferromagnetic state. That is, one could expect that the free-carrier screening becomes unimportant once the electron density becomes smaller than the one electron per the domain wall length L_{WF}. If we assume that this condition is satisfied at $T < 20$ K and take into account the resistance increase of about 5 orders of magnitude between RT and 20 K, we get for $L_{WF} \approx 100$ μm. As far as the temperature behaviour of the relaxation strength is concerned, a observed decrease might indicate that the domain walls are more restricted to move as the temperature lowers.

In what follows we address the origin of the magnetic ground state in the κ-(ET)$_2$Cl compound. The fact that the weak ferromagnetism is concomitantly established with the antiferromagnetic transition suggests that this phase transition is driven by the Dzyaloshinsky-Moriya (DM) interaction [13,14]. We recall that, AFMR modes observed in submillimeter wave AFMR measurements between 50 and 383 GHz might be well explained only if the DM interaction is taken into account [15]. This interaction implies that an anisotropic exchange interaction due to the spin-orbit coupling in the superexchange mechanism is present. In a two-sublattice model of antiferromagnetism, such an interaction will cant the sublattices toward one another and hence create a weak magnetic moment of the order of $\mid \mathbf{D} \cdot (\mathbf{M_1} \times \mathbf{M_2}) \mid$. $\mathbf{M_i}$ is the static sublattice magnetization, and $\mathbf{D}$ is a constant vector. When $\mathbf{D}$ is finite, a finite net magnetization sets in. The analysis of the magnetization measurements also show that in addition to the dipole-dipole interaction, spin-orbit coupling equally contributes to the magnetic anisotropy energy [10]. Namely, if only the former is taken into account, the easy axis is found to be parallel to the a-axis, contrary to the experimentally observed b-axis. The relevance of the spin-orbit coupling is usually considered to be very weak in organic materials. Nevertheless, BEDT-TTF contains 8 sulphur atoms leading to a strong intersystem crossing from the first excited singlet state to the lowest excited triplet state. This can be seen from the fact that the BEDT-TTF molecule shows no fluorescence, but strong phosphorescence [16]. Large intersystem crossing rates are a sign for a relatively strong spin-orbit coupling. In order to locate spin sites responsible for the magnetic structure, we have looked at the crystallographic structure of κ-ET$_2$Cu[N(CN)$_2$]Cl and searched for symmetry operations required by Dzyaloshinsky. Namely, Dzyaloshinsky has pointed out that the possible existence of this type of coupling might be determined from purely symmetry considerations. He has argued that the weak ferromagnetism would arise in the antiferromagnetic ground state if it is possible that the spin distribution symmetry of the former is identical with the spin distribution symmetry of the latter. In other words, symmetry considerations enable to decide whether ferromagnetism is possible in a given antiferromagnetic structure of a crystal and to find the direction of a ferromagnetic moment which is permissible in a given structure symmetry. In our case, the spins are parallel to b-axis in the antiferromagnetic spin arrangement, while a net magnetic moment in a canted spin arrangement lies in the ac-plane and is aligned along c-axis. We have checked four different symmetry rules given by Moriya, and found that only one rule is fulfilled. We consider the coupling between two ET dimers 1 and 2 located in adjacent donor layers at $y = 0$ (A) and $y = 1/2$ (B) (see Fig. 12). This rule implies that if a mirror plane exists which passes through the point bisecting the straight line AB, then $\mathbf{D}$ is finite and parallel with this mirror plane. Indeed, the anion-chain layer, that is to say, the plane located at $y = 1/4$, is the mirror plane in the space group $Pnma$ of the κ-ET$_2$Cu[N(CN)$_2$]Cl compound. Therefore, according to Moriya's rule, the coupling between sublattice magnetizations which favours the canted spin arrangement exists and should lie in the ac-plane. Taking into account that the spins are canted by a small angle from the b-axis and that the net moment vector $\mathbf{M_f}$ is aligned along c-axis, we conclude that $\mathbf{D}$ is aligned along a-axis.

Finally, we comment the observed high temperature anisotropy behaviour and the Debye relaxation mode. The former reveals the existence of the Curie-Weiss behaviour of the anisotropy in the large temperature range and an additional non-linear magnetization. This non-linear magnetization is not the usually known permanent magnetization, as the torque does not display $\sin(\varphi)$ dependence and does not reverse the sign when the field polarity is changed (see Fig. 2(b)). Its magnitude is anomalously enhanced by a subsequent thermal cycling between RT and 77 K. However, this cycling and the associated non-linear magnetization does not affect the phase transition at 22 K and the low-temperature canted antiferromagnetic state. This observation suggests that the non-linear magnetization cannot be due to the BEDT-TTF spin sites. Further, the observed high temperature increase of the anisotropy indicates a much larger change than one could expect from g-factor anisotropy associated with BEDT-TTF spin sites and measured by electron spin resonance [10], since the reported susceptibility shows a rather small temperature dependence. We point out that our static susceptibility measurements by the Faraday method [9], performed on samples from the same batch as our anisotropy measurements, reveal the same magnitude and the temperature behaviour of the susceptibility as reported in the literature [8,10]. Therefore, the high temperature anisotropy behaviour cannot be reconciled with the susceptibility behaviour which is associated with BEDT-TTF spins, and consequently cannot lead to the antiferromagnetic transition at $T_N = 22$ K to the weak ferromagnetic ground state.

We are tempted to attribute the non-linear magnetization and the Curie-Weiss behaviour of the anisotropy in the high temperature region to spins which belong to Cu sites in the anion channels. This assumption implies the existence of Cu^{2+} ions in the otherwise nonmagnetic Cu^{1+} anion lattice. We note that a distinct temperature behaviour of the anisotropies in the ab and bc-plane (see Fig. 1) is theoretically expected [17] if the single ion anisotropy is present, which is a reasonable assumption. If we assume that the observed anisotropy is due to the g-factor anisotropy of localized Cu^{2+} spins, and taking into account the Curie-Weiss temperature dependence, we get a few percents of Cu^{2+} spin sites. This estimate is somewhat surprising, since the Cu^{2+} contents reported so far in the κ-(BEDT-TTF)$_2$X samples have not exceeded 0.15% [18,19]. However, it is worth mentioning that several recent publications dedicated to the κ-(BEDT-TTF)$_2$X materials, where X is Cu[N(CN)$_2$]Cl, Cu[N(CN)$_2$]Br, $Cu_2(CN)_3$, in order to explain the results observed pointed to the presence of Cu^{2+} ions showing that its amount might depend on the sample preparation procedure [18–21]. If paramagnetic impurities or defects were the origin of cycling effects and of the Curie-Weiss behaviour observed we would expect to find smearing of the AF phase transition due to the presumably random impurity distribution. Such an effect was not found in the experiment. Furthermore, we also find a non-linear magnetization which is highly sample and thermal cycling dependent, while paramagnetic impurities are characterized by the linear response of magnetization in the magnetic field. The ferro-like features observed in the paramagnetic phase might be a manifestation of the magneto-electric effect originating form Cu^{2+} spins in the anion layers [17, 22]. The Debye dielectric relaxation might also have the origin in a domain structure of the Cu^{2+} subsystem. The fact that the response has a Debye form means that the low number of density of states contributes to this relaxation mode. Our estimate of Cu^{2+} sites indicates that the latter is a reasonable assumption. Finally, we point out that from a chemical point of view, a Cu^{2+} ion in the anion layers seems to be unfavourable, nevertheless, a mixed-valence state is certainly possible.

4 Conclusion

In summary, the BEDT-TTF spins in κ-(BEDT-TTF)$_2$-Cu[N(CN)$_2$]Cl become antiferromagnetically ordered with a canting arrangement at 22 K. A transition of this kind was anticipated over three decades ago by Dzyaloshinsky and Moriya. The easy axis is confirmed to be along the crystallographic b-axis. Our data reveal that the canting angle is $6 \cdot 10^{-2}$ degrees and that the vector of ferromagnetic magnetization is aligned along the crystallographic c-axis. The Dzyaloshinsky-Moriya vector, responsible for the finite net magnetization, is found to be aligned along the a-axis. Further, the hysteresis in the spin-flop transition and magnetic field reversal of the ferromagnetic magnetization, observed for the first time, are features not known in the standard antiferromagnets and spin density waves. The observed Curie-Weiss anisotropy behaviour, as well as the observed rare type of non-linear field-induced magnetization in the high-temperature region, appear to be associated with spin sites different than BEDT-TTF and therefore cannot be the origin of this phase transition. The low-frequency dielectric response indicates that two length scales and two time scales are involved in the problem. We identify broad relaxation as the intrinsic property of the weak ferromagnetic state below 22 K and suggest a charged domain wall in the random domain structure as the relaxation entity. We speculate that the Debye relaxation and the high-temperature ferro-like magnetization might be the manifestations of the magnetoelectric effect linked to a Cu^{2+} subsystem.

To our knowledge this might be the first opportunity to study experimentally the theoretically intriguing issue of the dynamics of the magnetically ordered domain structure in a layered organic conductor. Further measurements of the angular and temperature dependence of the torque at different magnetic fields are planned.

Acknowledgements

This work was partially supported by the Croatia-Germany bilateral collaboration project, ref. KRO-020-95.

References

1. *Organic Conductors*, edited by J. P. Farges, Series Applied Physics (Marcel Dekker, Inc., New York, 1994).
2. *Organic Superconductors*, edited by T. Ishiguro and K. Yamaji, Springer Series in Solid-State Sciences (Springer Verlag, Berlin Heidelberg 1990) 88.
3. J. M. Williams et al., Inorg. Chem.**29**, (1990) 3272.
4. J. E. Schirber, D. L. Overmyer, K. D. Carlson, J. M. Williams, A. M. Kini, H. H. Wang, H. A. Charlier, B. J. Love, D. M. Watkins and G. A. Yaconi, Phys. Rev. B **44**, (1991) 4666.
5. U. Welp, S. Fleshler, W. K. Kwok, G. W. Crabtree, K. D. Carlson, H. H. Wang, U. Geiser, J. M. Williams and V. M. Hitsman, Phys. Rev. Lett. **69**, (1992) 840.
6. K. Miyagawa, A. Kawamoto, Y. Nakazawa and K. Kanoda, Phys. Rev. Lett. **75**, (1995) 1174.
7. H. Kino and H. Fukuyama, J. Phys. Soc. Jpn **64**, (1995) 2726.
8. A. Kawamoto, K. Miyagawa, Y. Nakazawa and K. Kanoda, Phys. Rev.**B52**, (1995) 15522.
9. M. Miljak et al., unpublished.
10. M. Kubota, G. Saito, H. Ito, T. Ishiguro and N. Kojima, Mol. Cryst. Liq. Cryst. **284**, (1996) 367.
11. S. Havriliak and S. Negami, J. Polym. Sci. C **14**, (1966) 99.
12. R. J. Cava, R. M. Fleming, R. G. Dunn and E. A. Rietman, Phys. Rev. B **31**, (1985) 8325.
13. I. Dzyaloshinsky, J. Phys. Chem. Solids **4**, (1958) 241.
14. T. Moriya, Phys. Rev. **120**, (1960) 91.
15. H. Ohta, S. Kimura, Y. Yamamoto, J. Azuma, K. Akioka, M. Motokawa and K. Kanoda, Synth. Metals **86**, (1997) 2079.
16. H. Grimm, D. Schweitzer and K. H. Hausser, Proceedings of the XXIII Congress Ampere on Magnetic Resonance, Roma 1986, ed. by B. Moraviglia, F. De Luca and R. Campanella, Instituto Superiore di Sanita, Roma (p228).
17. T. Moriya in *Magnetism*, edited by G. T. Rado and H. Suhl, vol. 1. (Academic Press Inc., New York 1963), 85-125.
18. T. Komatsu, N. Matsukawa, T. Inoue and G. Saito, J. Phys. Soc. Jpn.**65**, 1340 (1996).
19. L. K. Montgomery, R. M. Vestal, K. P. Starkey, B. W. Fravel, M. J. Samide, D. G. Peters, C. H. Mielke and J. D. Thompson, Proceedings of the International Conference on Science and Technology of Synthetic Metals, Montpellier, July 12-18, 1998, France.
20. C. H. Mielke, N. Harrison, D. G. Rickel, A. H. Lacerda, R. M. Vestal and L. K. Montgomery, Phys. Rev. B **56**, (1997) RC4309.
21. M. A. Tanatar, T. Ishiguro, H. Ito, M. Kubota and G. Saito, Phys. Rev. B **55**, (1997) 12529.
22. H. Wiegelmann, A. A. Stepanov, I. M. Vitebsky, A. G. M. Jansen and P. Wyder, Phys. Rev. B **49**, (1994) 10039.